

Article

Analyzing of a Photovoltaic/Wind/Biogas/Pumped-Hydro Off-Grid Hybrid System for Rural Electrification in Sub-Saharan Africa—Case Study of Djoundé in Northern Cameroon

Nasser Yimen *, Oumarou Hamandjoda, Lucien Meva'a, Benoit Ndzana and Jean Nganhou

National Advanced School of Engineering, University of Yaoundé I, POB: 8390, Yaounde, Cameroon; oumahama@yahoo.com (O.H.); jrl67_mevaa@yahoo.com (L.M.); bendzana@yahoo.fr (B.N.); jean.nganhou@yahoo.com (J.N.)

* Correspondence: nazerois@yahoo.fr; Tel.: +237-670-147-046

Received: 12 September 2018; Accepted: 28 September 2018; Published: 3 October 2018



Abstract: Traditional electrification methods, including grid extension and stand-alone diesel generators, have shown limitations to sustainability in the face of rural electrification challenges in sub-Saharan Africa (SSA), where electrification rates remain the lowest in the world. This study aims at performing a techno-economic analysis and optimization of a pumped-hydro energy storage based 100%-renewable off-grid hybrid energy system for the electrification of Djoundé, which is a small village in northern Cameroon. Hybrid Optimization of Multiple Energy Resources (HOMER) software was used as an analysis tool, and the resulting optimal system architecture included an 81.8 kW PV array and a 15 kW biogas generator, with a cost of energy (COE) and total net present cost (NPC) of €0.256/kWh and €370,426, respectively. The system showed promise given the upcoming decrease in installation cost of photovoltaic systems. It will be viable in parts of SSA region but, significant investment subsidies will be needed elsewhere. The originality of this study can be emphasized in three points: (1) the modelling with the recently introduced pumped-hydro component of HOMER; (2) broadening sensitivity analysis applications to address practical issues related to hybrid renewable energy systems (HRES); and, (3) consideration of the agricultural sector and seasonal variation in the assessment of the electricity demand in an area of SSA.

Keywords: hybrid renewable energy system; pumped-hydro energy storage; off-grid; optimization; HOMER software; rural electrification; sub-Saharan Africa; Cameroon

1. Introduction

Energy, especially electricity, is a vital commodity for everyday life in the contemporary world. It is the primary driver for any human, social, or economic development. However, electricity is still a luxury in many places around the world [1]. According to the International Energy Agency (IEA) [2], 1.1 billion people viz. 14% of the world's population did not have access to electricity in 2016. The issue was especially acute in Sub-Saharan Africa (SSA) where 588 million people needed access to electrical energy. The rural electrification rate in the region was only 23%, as compared with 71% in urban areas. This rate was unequally distributed, as illustrated by the electrification rates of selected countries shown in Figure 1. While some countries, such as Ethiopia and Kenya, have experienced rural electrification above 50%, others, such as Chad and Mauritania, have achieved less than 5%. The situation is particularly worrying because over 60% of the regional population lives in rural areas. This is an obstacle to political change, job creation, social welfare, economic growth, the modernization

of education, the adoption of modern agricultural technology, and the promotion of gender equality, as demonstrated in [3–6].

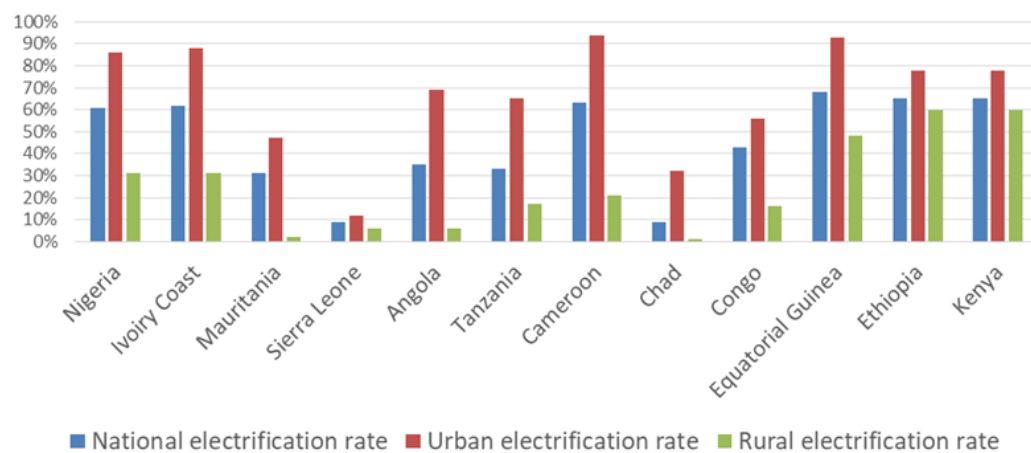


Figure 1. Electrification rates of some Sub-Saharan African (SSA) countries.

The grid extension has long been the primary means of electrification of the region. However, connection to the grid is most of the time practically impossible due to geographical remoteness, thick jungles, rugged terrains, high costs of supply, low household incomes, low consumptions, dispersed settlement of consumers, and inadequate road infrastructures [7]. As a result, decentralized diesel generators are most often used for rural electrification in the region. However, the high costs that are associated with the transportation of fuels and the maintenance of those systems make them unsuitable for rural electrification in developing countries. On a world basis, fossil fuel resources are experiencing a rapid depletion, resulting in an ever-increasing price which tends to make them unaffordable for developing nations. The growing evidence of global warming phenomena due to the release of greenhouse gases when burning those fuels is another critical reason for reducing our dependence on them [8]. Therefore, finding alternative energy sources to meet the growing energy demand while minimizing adverse environmental impacts is becoming an imperative task.

Renewable energy sources, namely solar, wind, biomass, geothermal, and hydro, being inexhaustible, locally available, free, and eco-friendly can constitute potential sources of alternative energy, especially for local power generation in remote rural areas. Increasing interest has been given to their utilization since the oil crises of the 1970s [9].

The main drawbacks associated with the utilization of renewable energy sources are their unreliability and inability to work efficiently due to their intermittent and fluctuating nature, which generally leads to the over-sizing of the system, thereby increasing the investment cost. The hybrid renewable energy systems (HRES) have recently gained popularity as an effective means to deal with the disadvantages that are related to single source based renewable energy systems. A hybrid system is made up of two or more power generation plants fed with appropriate fuels (renewable or fossil fuel) along with energy storage and electronic appliances. The main advantages of hybrid renewable energy systems over single-source systems include [10]:

- higher reliability,
- better efficiency,
- reduced energy storage capacity, and
- lower levelized life-cycle power cost.

For developing countries, the literature on hybrid renewable energy systems is dominated by optimal design studies. The main problem addressed in those studies is to find the appropriate size or number of each component constituting the system, so as to maximize/minimize the objective

functions and satisfy all constraints. Many approaches and software tools have been used to handle the issue, as mentioned above.

Reviewing all of the research carried out in this area is beyond the scope of this paper. However, for an indicative purpose, we only mention some, notably the analysis conducted by Nfah and Ngundam [11] on a pico-hydro (PH)/PV hybrid system incorporating a biogas generator and a battery for remote areas of Cameroon. Using HOMER software the authors simulated the system and determined the optimal configurations for localities in the Southern and Northern regions. The cost of energy (COE) and breakeven grid distance were determined at 0.352 €/kWh and 12.9 km and at 0.395 €/kWh and 15.2 km, respectively, for southern and northern locations. Adaramola et al. [12] used HOMER to perform the techno-economic optimization of a solar/wind/Diesel Generator (DG) hybrid energy system in remote areas of Ghana. Considering the levelized cost of electricity (LCOE) and the net present cost (NPC) as the performance criteria, they found out that the optimal system was made up of an 80 kW PV array, a 100 kW wind turbine, and a 600 Surrette 4KS25P, and produced 791.1 MWh of electricity yearly at the cost of \$0.281/kWh. Halabi et al. [13] used Homer to model and simulate a PV/diesel/battery HRES to meet domestic electricity needs in Sabah, Malaysia. They found that the optimized system's NPC and COE were \$5,571,168 and 0.311 \$/kWh, respectively, and its economic and technical performance was better than that of the existing standalone diesel generator and a hypothetical PV/Battery system. Singh et al. [14] used a swarm based artificial bee colony algorithm to find the optimal configuration of a hybrid PV/Wind/Biomass/battery system that is designed to meet the electricity demand of Patiala, an island village of India. They found that the optimal hybrid system was made up of a 250-kW PV array, 18 wind turbines of 1 kW, a biomass generator of 40 kW, and a 1.4-kWh battery, and it had an NPC and COE of \$7,230,378 and 0.173 \$/kWh, respectively. The system configuration analyzed by the previous authors was the focus of the study by Sigarchian et al. [15], who used HOMER software to perform techno-economic feasibility of using a biogas generator fuelled by locally produced biogas as a backup engine in comparison with using a diesel engine for the same purpose. The results showed that the NPC and COE of the optimized hybrid system with a biogas generator were, respectively, 18% and 20% lower than those of the system with a diesel generator. Baghdadi et al. [16] were interested in the design and simulation of a hybrid PV/Wind/Diesel/battery system to satisfy the power requirement of Adrar, a location in southern Algeria. They considered the renewable fraction as the performance criterion to be minimized and used HOMER software to perform the analysis which revealed that the renewable fraction of such a system could reach 70%. Ma et al. [17] investigated on a hybrid PV/Wind system integrated with a pumped hydro storage (PHS) to meet the domestic electricity demand of a hypothetical island in Hong Kong, China. They developed a mathematical model to simulate dozens of cases with different component capacities. They then focused on a technically feasible case made up of 110-kWp PV arrays, two wind turbines of 10.4 kW, and a pumped hydro storage system with a 5106-m³ upper reservoir. Finally, they concluded that PHS is the best energy storage system for 100% energy autonomy in islanded communities. Kenfack et al. [18] used HOMER software to investigate a hybrid PV/Micro-hydro/Battery system in Batocha, Cameroon. The analysis revealed that the optimal system to meet the electricity demand of the location was made up of a 5-kW PV array, a 2.12-kW Hydro plant, a 1-kW diesel generator and 125 units of a 24-Ah battery. The NPC and COE of the optimized system were estimated at \$70,042 and \$0.278/kWh, respectively. Singh and Fernandez [19] carried out analyses on a Photovoltaic-Wind-Battery hybrid system in Almora, a remote village of India. They used the MATLAB programming environment to implement Cuckoo Search, a new meta-heuristic algorithm for solving the optimization related problem of the system. They found that the NPC and LCOE of the optimized system were Rs 7.69 lakhs and 18.38 Rs/kWh, respectively. Ahmad et al. [20] performed a techno-economic optimization analysis on a wind-photovoltaic-biomass hybrid renewable energy system for rural electrification of Kallar Kahar, a Pakistani village. The researchers used HOMER for their study and found that the optimal system that was made up of a 15 MW PV array, a 15 MW wind farm, and a 20 MW biomass generator, had an NPC of \$180,290,247.40 and an LCOE of 0.05744 \$/kWh. Kusakana [21] developed the appropriate

mathematical model to simulate and optimize a hydrokinetic/diesel/Pumped-Hydro-Storage hybrid system to meet the energy demand of a hypothetical South African village, while considering daily diesel fuel consumption as the objective function to be minimized. They used MATLAB to implement the model that was developed, and found that such a system could help reduce daily operating costs by 88% when compared to a stand-alone diesel generator. Sawle et al. [22] went further by considering simultaneously technical, economic and social performance criteria through a new multi-objective function in the analysis of a HRES integrating wind, PV, biomass, diesel generator, and battery bank for the electrification of remote Indian areas. The authors used evolutionary optimization techniques and found that the PV/Biomass/Diesel/Battery configuration was the most efficient.

Table 1 summarizes all of the studies mentioned above. This summary highlights the fact that most of the HRES-based studies focused on meeting the demand for domestic and community electricity in rural areas and those that take into account the agricultural sector are rare. To the best of the authors' knowledge, such an application has never been performed in the SSA region, where the agricultural sector accounts for an average of 15% of GDP and employs more than 50% of the labor force, particularly in rural areas [23]. Also, the influence of the changes in weather and seasons on electricity consumption has never been taken into account in an HRES-based study in sub-Saharan Africa. Most SSA countries experience two types of seasons: the rainy season and dry season. Furthermore, it is clear from the literature review that the HOMER software is the most preferred tool for HRES analysis and that battery systems are the most used storage devices. However, battery storage systems have some disadvantages that make them less suitable than pumped hydro storage systems for HRES applications in sub-Saharan Africa. They contain lead and sulphuric acid, which entails risks of explosion and environmental degradation, as well as the need for recycling after use [24]. Besides, a study conducted in [25] shows that PHS systems have a lower lifecycle cost (LCC) than batteries. However practical cases of PHS-based HRESs are extremely rare in the literature. Given the advantages of PHS over batteries mentioned above, PHS-based HRESs may be more technically and economically efficient. Therefore, the modelling and analysing of these systems will help to clarify this hypothesis and promote the use of this energy storage technology in HRES systems. Early versions of HOMER did not include any specific PHS component in the storage component library. Recently, HOMER has introduced a generic 245 kWh PHS component. To the best of our knowledge, up to this point, no study has used this component to model a pumped hydro energy storage system. Besides, most of the previous studies that performed sensitivity analysis did not provide practical interpretations of their results. These interpretations are essential to better understand many aspects of HRESs in order to ensure their sustainable promotion for rural electrification.

The present study intends to fill the previously mentioned literature gaps by using HOMER software to analyze a PV/Wind/Biogas/PHS hybrid renewable energy system to meet domestic, community, commercial, and agricultural electricity needs of Djoundé, a remote location of Northern Cameroon.

The remainder of this paper is structured as follows. The next part, Section 2, introduces the materials and methods adopted to carry out the study. The results obtained are presented in Section 3, followed by Section 4, the discussion part. The paper ends with a conclusion in Section 5.

Table 1. Selected studies on hybrid renewable energy systems (HRES) in developing countries.

S No	Authors/Ref.	Country of Application	Energy Sources	Storage Device	Load Type	Study Objectives	Technique/Software
1	Nfah et al. [11]	Cameroon	MHP-SPV-BGS	Battery	DS	Minimizing NPC	HOMER
2	Adaramola et al. [12]	Ghana	WES-SPV-DG	Battery	DS	Minimizing NPC	HOMER
3	Halabi et al. [13]	Malaysia	SPV-DG	Battery	DS	Minimizing NPC	HOMER
4	Singh et al. [14]	India	SPV-WES-BGS	Battery	DS, C	Minimizing NPC	ABC algorithm
5	Sigarchian et al. [15]	Kenya	SPV-WES-BGS	Battery	DS	Minimizing NPC	HOMER
6	Baghdadi et al. [16]	Algeria	WES-SPV-DG	Battery	DS	Maximise the RF	HOMER
7	Ma et al. [17]	China	WES-SPV	PHS	DS, C	Finding a feasible configuration	Mathematical models
8	Kenfack et al. [18]	Cameroon	SPV-MHS	Battery	DS, C	Minimizing NPC	HOMER
9	Singh and Fernandez [19]	India	WES-PV	Battery	DS, C	Minimizing NPC	MATLAB & Cuckoo Search
10	Ahmad et al. [20]	Pakistan	WES-PV-BMS	No SD	DS, C	Minimizing NPC	HOMER
11	Kusakana [21]	South Africa	HKN-DG	PHS		Maximise the RF	MATLAB
12	Sawle et al. [22]	India	WES-PV-BMS-DG	Battery	DS, C	Multi objective	Genetic algorithm

Note: ABC: Artificial Colony Bee; BGS: Biogas Generating System; BMS: Biomass Generating System; C: Commercial; DG: Diesel Generator; DS: Domestic Sector; MHP: Micro Hydropower; PHS: Pumped Hydro System; RF: Renewable fraction; SD: Storage Device; SPV: Solar Photovoltaic; WES: Wind Energy System.

2. Materials and Methods

2.1. Introduction

Two main approaches for analysing and optimizing HRES have been reported in the literature: optimization techniques and software tools. A thorough review of all these methods is given in [26,27]. Software tools that include, among others, HOMER, HIBRID2, and HOGA, have received increasing attention in the literature given the dramatic improvement in computing power of modern computers. The Hybrid Optimization of Multiple Energy Resources (HOMER), initially developed in 1992 at the National Renewable Energy Laboratory (NREL) in the United States of America (USA), appears to be the most widely used tool in light of the literature review above. It is available in two classes of versions: HOMER Legacy (free) and HOMER Pro (commercial), and it can perform simulations, optimizations, and sensitivity analyses. Besides, its library includes a wide range of technologies and components that make it handy for modelling HRES. These merits have justified the choice of HOMER in its latest version, HOMER Pro Version 3.12.1, as an analysis tool. Further information about its operational mode is provided in [28]. Analyses were performed on Windows 10 Pro 64-bit with 2 GHz Intel Core i7 CPU, 8 GB of RAM, and 3 GB GPU.

The block diagram of the adopted research methodology is illustrated in Figure 2. HOMER software was complemented by a pre-HOMER phase, including a detailed assessment of the village load, available resources, and site layout. During this phase, information collected through surveys, expert opinions, and literature reviews was analysed to obtain data adapted to HOMER in addition to other technical and economic parameters. Detailed information on the methodology is given in the following subsections.

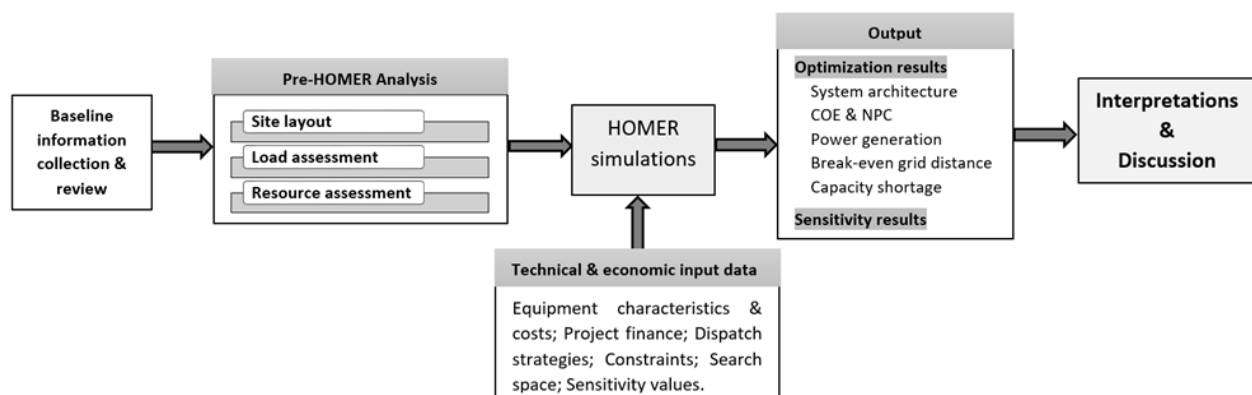


Figure 2. Block diagram of research methodology.

2.2. Study Location

The autonomous hybrid system to be designed was intended to meet the electricity needs of. The village is one of the localities of Cameroon not yet connected to the national electricity grid. Figure 3 shows the geographical situation of the study location, while the related background information is displayed in Table 2.



Figure 3. Geographical situation of the study location.

Table 2. General information about the study location.

Particulars	Details
Country	Cameroon
Region	Far North
Division	Mayo-Sava
Name of the municipality	Mora
Latitude	11°03'00" North
Longitude	14°18'00" East
Elevation above sea level	100 m
Number of households	180
Nearest power transformer	Mora, 18 km
Main socio-economic activities	Agriculture, small business, and crafts

2.3. Load Assessment

The electricity needs of remote rural areas are generally lower than those of urban areas. In this study, the demand for electrical energy at the study site was assessed on the basis of a survey taking into account the future needs of the village as well as expert opinion and previous cases implemented in Pakistan and India [29,30]. The rating and the number of energy-consuming appliances needed for the 180 households in the village, as well as all other sectors considered are shown in Table 3. The two seasons that prevail in the study areas, namely the rainy season (May to September) and the dry season (October to April), affect the energy consumption of some devices, such as fans and irrigation pumps. In fact, the temperatures in the rainy season are lower than those in the dry season, so that most of the time, the fans are not used during the rainy season. Moreover, thanks to the rain that falls during the rainy season, less water is required for irrigation. Consequently, the hourly power demand of the study location was evaluated separately for the two seasons, as presented in Table 4. The daily electricity demand of the study area during dry and rainy seasons were determined at 381.07 kWh/day and 302.23 kWh/day, respectively, for an annual average of 348.02 kWh/day. The annual electricity demand was evaluated at 127,027 kWh/year. Day-to-day variability of 20% and time-step-to-time-step

variability of 15% were considered to make the load profile more realistic. The peak power and load factor were, respectively, 57.88 kW and 0.25. The seasonal load profile is shown in Figure 4.

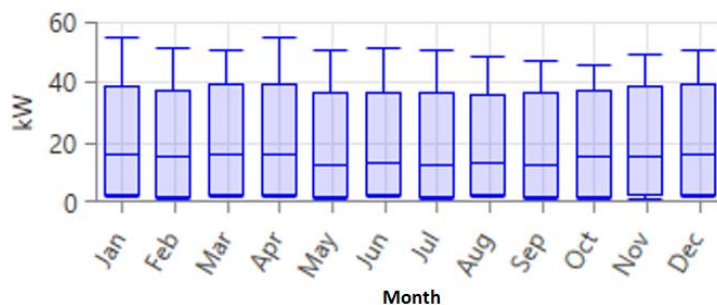


Figure 4. The seasonal load profile of the study location.

Table 3. Appliances' requirement and rating for different sectors of energy consumption.

Load Type	Appliances	Rating (W)	Total Quantity
A-Domestic			
	CFL	15	360
	TV	65	180
	Radio	12	180
	Mobile Charger	12	180
	Fan	40	360
	Water pump	450	9
B-Commercial			
Shops	CFL	15	12
	Fan	40	12
	Refrigerator	500	1
Mini dairy	-	3000	1
Flour mill	-	4800	1
C-Agricultural			
Water irrigation pumps	-	2200	3
Cutting machine	-	1500	2
Threshing machine	-	4000	2
D-Community			
School	CFL	15	20
	Fan	40	2
	CFL	15	5
Health centre	Fan	40	6
	Refrigerator	500	1
Street lights	CFL	100	20

Note: CFL: Compact Fluorescent Lamp.

Table 4. Hourly electricity demand of the study location during dry and rainy seasons.

Hour	Domestic load (kW)				Commercial Load (kW)				Agricultural Load (kW)				Community Loads				Electricity Demand (kW)							
	CFL		TV	Radio	Fan DS/RS	WP	MC	CFL	Fan DS/RS	RF	FM	MD	WIP DS/RS	TM	CM	CFL	Fan DS/RS	CFL	Fan DS/RS	RF	STL	Dry Season	Rainy Season	
01:00										0.5							0.075		0.5	2	3.075	3.075		
02:00										0.5							0.075		0.5	2	3.075	3.075		
03:00										0.5							0.075		0.5	2	3.075	3.075		
04:00	5.4		2.2							0.5							0.075		0.5	2	10.675	10.675		
05:00	5.4		2.2			2.2				0.5						3		0.075		0.5	2	15.875	15.875	
06:00			2.2			2.2				0.5		3				3		0.075		0.5		11.475	11.475	
07:00						2.2				0.5		3				3	0.6	0.8/0	0.075		0.5		10.675	9.875
08:00										0.5		3					0.6	0.8/0		0.5			5.4	4.6
09:00										0.5							0.6	0.8/0		0.5			2.4	1.6
10:00										0.5							0.6	0.8/0		0.5			2.4	1.6
11:00					7.2/0					0.5	4.8						0.6	0.8/0	0.24/0	0.5			14.64	6.4
12:00			2.2	7.2/0						0.48/0	0.5	4.8					0.6	0.8/0	0.24/0	0.5			17.32	8.6
13:00			2.2	7.2/0						0.48/0	0.5			6.6/6.6			0.6	0.8/0	0.24/0	0.5			19.12	10.4
14:00	11.7	2.2	7.2/0							0.48/0	0.5			6.6/0			0.6	0.8/0	0.24/0	0.5			30.82	15.5
15:00	11.7	7.2/0								0.48/0	0.5				8		0.6	0.8/0	0.24/0	0.5			30.02	21.3
16:00	11.7	7.2/								0.48/0	0.5				8				0.24/0	0.5			28.62	20.7
17:00	11.7	7.2/0								0.48/0	0.5								0.24/0	0.5			20.62	12.7
18:00	5.4	11.7	7.2/0						0.18	0.48/0	0.5							0.075		0.5	2	28.035	20.355	
19:00	5.4	11.7	2.2			9			0.18	0.48/0	0.5							0.075		0.5	2	32.035	31.555	
20:00	5.4	11.7	2.2			9			0.18	0.48/0	0.5							0.075		0.5	2	32.035	31.555	
21:00	5.4	11.7	2.2			9			0.18	0.48/0	0.5							0.075		0.5	2	32.035	31.555	
22:00	5.4	11.7							0.18	0.48/0	0.5							0.075		0.5	2	20.835	20.355	
23:00									0.18	0.48/0	0.5							0.075		0.5	2	3.735	3.255	
00:00										0.5								0.075		0.5	2	3.075	3.075	

Note: CFL: Compact Fluorescent Lamp; CM: Cutting machine; DS: Dry season; FM: Flour mill; MC: Mobile charger; MD: Mini dairy; RF: Refrigerator; RS: Rainy season; STL: Street lights; TM: Treshing machine; TV: Television; WIP: Water irrigation pump; WP: Water pump; WS: Wet season.

2.4. System Configuration

The schematic diagram of the system involved in this study is presented in Figure 5. The system is equipped with three power generators (PV array, biogas generator, and wind turbine); an energy storage device, the pumped hydro storage (PHS); a converter system; a control station; and, a load.

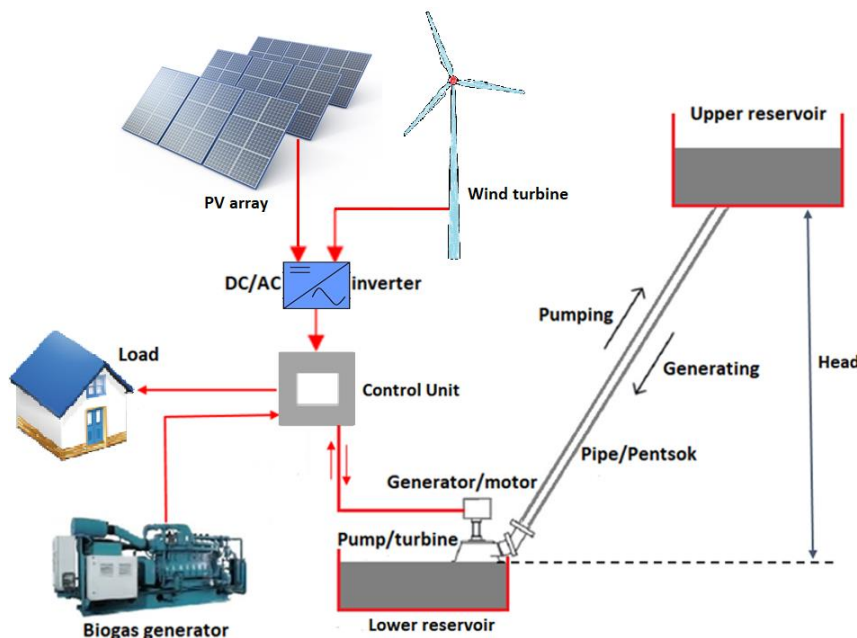


Figure 5. The schematic diagram of the hybrid renewable energy system.

The PHS stores excess electricity from intermittent sources in the system (PV and wind) for use during periods of insufficient generation to meet the demand for electrical load. The operating principle of the pumped hydro system can be explained briefly, as follows. During a period of excess energy supply, the surplus wind or PV power is used to pump and raise water from the lower reservoir to the upper reservoir. Later, when a supply-demand imbalance occurs, the stored water is allowed to return to the lower reservoir, thus enabling electricity production through a turbine/generator unit [31]. The biogas generator is used as a backup power source to be activated in case of insufficient combined production from PV array, wind turbine and PHS. The proposed system as implemented by the HOMER software is illustrated in Figure 6. The pumped hydro storage, which is in fact an AC component, is connected to the DC bus in HOMER. Indeed, HOMER models the PHS component as a special battery with an initial and minimum state of charge of 100% and 0%, respectively. The consequence of this modelling is the need for a rectifier in the HOMER model, although this is not necessary in the actual configuration of the system. The aim of the rectifier in HOMER's model is to convert the surplus AC output from the biogas generator to DC current to be stored by the storage device in case of cycle charging dispatch strategy. The system is an off-grid system, i.e., it is not connected to the grid. The grid component on the HOMER's schematic presentation was introduced for the purpose of comparing the proposed autonomous system with the grid extension.

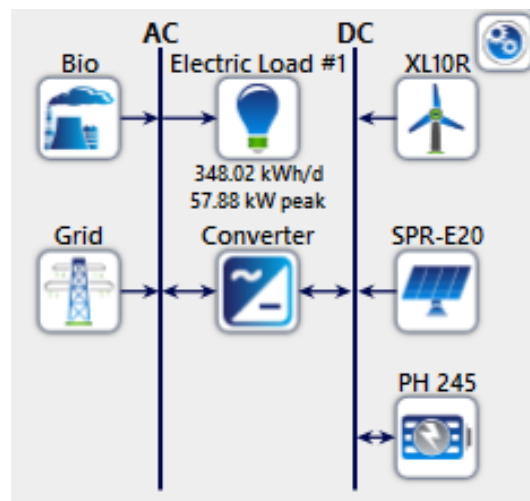


Figure 6. The proposed hybrid system in Hybrid Optimization of Multiple Energy Resources (HOMER).

2.5. Assessment of Available Energy Resources

2.5.1. Available Solar and Wind Resources

Data on solar radiation and wind speed in Djoundé, the study location, were collected from the NASA Surface meteorology and Solar Energy (SSE) database [32] at the coordinates of Mora ($11^{\circ}03'00''$ N, $14^{\circ}18'00''$ E), the closest data location. The annual average solar radiation was found to be $5.82 \text{ kWh/m}^2/\text{day}$, while the average clearness index was 0.6. The maximum solar irradiation, $6.67 \text{ kWh/m}^2/\text{day}$, is that of March whereas the minimum, $4.77 \text{ kWh/m}^2/\text{day}$, is that of August. Figure 7 displays the monthly daily average solar radiation and the clearness index of the selected location. It was generated by HOMER after SSE data entry. It highlights the high potential of the area for solar energy that can be used to generate electricity through PV arrays.

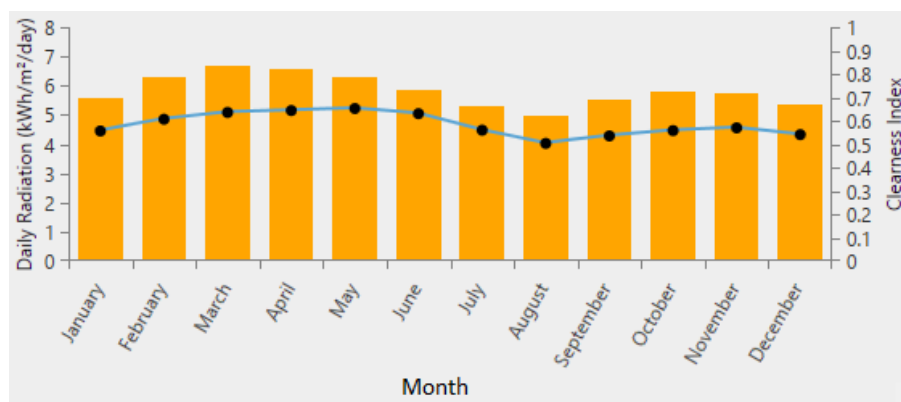


Figure 7. The monthly daily average solar radiation and clearness index for Djoundé.

Monthly data on mean wind speed are shown in Figure 8. The average annual wind speed at the site was 4.95 m/s at the 50 m anemometer. A study by Kidmo et al. [33] showed that the high altitude above the sea level makes the site fruitful for wind power production, despite the relatively low wind speed recorded.

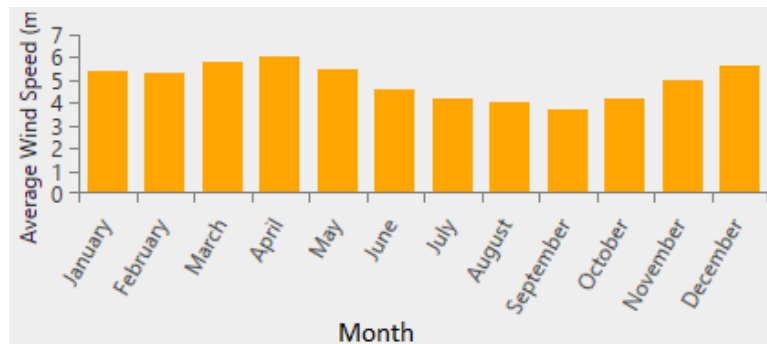


Figure 8. The average monthly wind speed measured at 50 m in Djoundé.

2.5.2. Biomass Resources

Biomass refers to all organic materials that can be converted into energy. It includes both materials of plant origin (agricultural residues, leaves, wood) and those of animal origin (animal and human wastes, living beings of the soil, animal corpses). In this study, livestock manure was considered to be the only biomass resource for power generation. The data filled in HOMER was the average daily manure available for biogas production. Based on the survey conducted in the study area, the total livestock population was 811, consisting of cows (213), horses (12), mules (29), and goats (557). Table 5 provides a detailed assessment of the potential for generating biogas and electricity from on-site livestock manure. The evaluation of the biogas was carried out on the basis of manure yield. For that, we assumed a daily manure production of 10 kg/day for any cow/mule/horse and 1 kg /day for any goat [34]. When considering a recovery factor of 0.7 and a "gas yield per kg of wet manure" of 0.036 m³/kg [35], the total biogas yield was determined at 78 m³/day. Finally, given that 0.73 m³ of biogas is needed to produce 1 kWh of electricity [36], the total potential for producing electricity from the livestock manure produced on site was 107 kWh/day. As inputs for biomass resources, HOMER requires the cost of biomass, gasification ratio (GR), and lower heating value (LHV). The gasification ratio indicates the amount of biogas produced per unit mass of biomass, while the LHV is the amount of energy contained in 1 kg of biogas available to feed the biogas generator. In this study, the GR and LHV were 0.05 kg/kg and 5.5 MJ/kg, respectively [37]. The cost of biomass was set at 0 €/t.

Table 5. Electricity potential from biomass of the study area.

Livestock	Population	Dung Availability (kg/head/day)	Total Dung (kg/day)	Total Dung (Recovery Factor = 0.70)	Total Gas Yield (m ³ /day)	Potential Power Yield (kWh/day)
Cows	213	10	2130	1491	53.7	74
Horse	12	10	120	84	3	4
Mule	29	10	290	203	7.3	10
Goat	557	1	557	390	14	19
Total	811	-	3097	2168	78	107

2.6. System Analysis

2.6.1. PV Array

The model of PV solar module adopted in this study was SPR-E20-327, a monocrystalline module manufactured by Sunpower. The module has a rated power of 327 W_p and it can produce a maximum voltage of 600 V DC. Table 6 presents the technical specifications of the selected PV module. The following equation is used by HOMER to calculate the output of a PV array [38]:

$$P_{output} = \gamma_{PV} f_{PV} \left(\frac{G_T}{G_{T,STC}} \right) [1 + \alpha_P (T_c - T_{c,STC})], \quad (1)$$

where, f_{PV} is the PV derating factor (%), Y_{PV} the rated capacity of the PV array (kW), G_T the global solar radiation incident on the surface of the PV array (kW/m^2), and $G_{T,STC} = 1 \text{ kW}/\text{m}^2$ is the standard amount of incident radiation at the standard test condition (25°C), α_p is the temperature coefficient of power (%/ $^\circ\text{C}$), T_c is the PV cell temperature, and $T_{c,STC}$ is the PV cell temperature under the standard test condition. HOMER uses the Graham and Hollands algorithm to generate hourly global solar radiation from the monthly average global solar radiation [39]. The temperature coefficient of power for the selected module is $-0.38\%/\text{ }^\circ\text{C}$, as shown in Table 6 of the technical specifications of the said PV module. A derating factor of 0.95 was considered in this study. The lifespan of the PV generator is assumed to be 25 years. The total capital cost, replacement cost, and operation and maintenance cost for the PV installation were estimated at $3000 \text{ €}/\text{kW}$, $3000 \text{ €}/\text{kW}$, and $10 \text{ €}/\text{kW}/\text{year}$ [40].

Table 6. PV module specifications [41].

Item	Specification
Manufacturer	Sunpower
PV Module type	Mono-si
Module number	SPR-E20-327-C-AC
Module efficiency	20.4%
Power capacity	327 W
Power tolerance	+5/-0%
Rated voltage (Vmpp)	54.7 V
Rated current (Impp)	5.98 A
Open-Circuit Voltage (VoC)	64.9 V
Short-Circuit Current (ISC)	6.46 A
Maximum system voltage	DC 600 V
Power Temp Coef	$-0.38\%/\text{ }^\circ\text{C}$
Volt Tem coef	$-175 \text{ mV}/\text{ }^\circ\text{C}$
Current Temp Coef	$3.5 \text{ mA}/\text{ }^\circ\text{C}$
Dimensions	46 mm \times 1559 mm \times 1046 mm
Operating temperature	-40°C to $+85^\circ\text{C}$
Area	1.63 m^2
Weight	18.60 kg

2.6.2. Wind Turbine

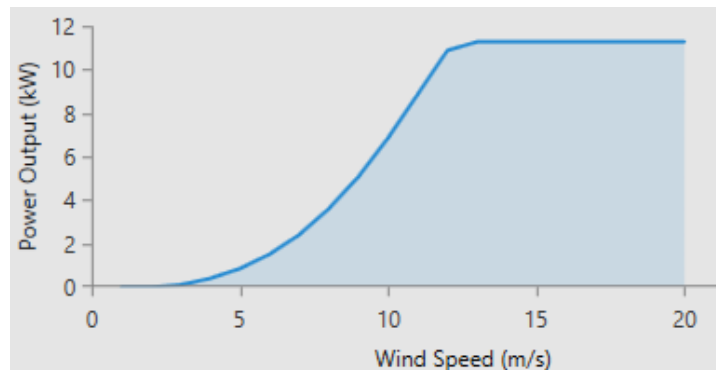
The wind turbine model that is considered for this study is the bergey excel 10-R model, manufactured by Bergey Windpower. Its nominal power is 10 kW at 12 m/s. The technical specifications of the turbine are presented in Table 7, while its power curve is shown in Figure 9. The power law was used to calculate wind speed at the hub height [12]:

$$U_{hub} = U_{anem} \cdot \left(\frac{Z_{hub}}{Z_{anem}} \right)^\alpha, \quad (2)$$

where, U_{hub} and U_{anem} are the wind speeds at the hub and anemometer height (Z_{hub} , and Z_{anem}), and α is the power law exponent whose the typical value for low roughness site is 0.14 [15]. The total initial cost, replacement cost, and operation and maintenance cost were estimated at $50,000 \text{ €}/\text{unit}$, $30,000 \text{ €}/\text{unit}$, and $200 \text{ €}/\text{year}$ [40]. The turbine lifespan was assumed to be 20 years.

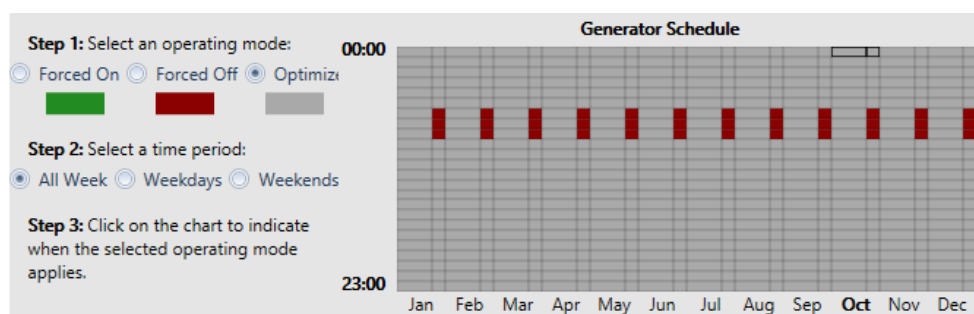
Table 7. Technical specifications of the selected wind turbine model [42].

Item	Specification
Manufacturer	Bergey WindPower
Model	Bergey excel 10-R
Nominal power	10 kW at 12 m/s
Cut-in Wind Speed	2.5 m/s
Cut-Out Wind Speed	None
Furling Wind Speed	14–20 m/s
Max. Design Wind Speed	60 m/s
Temperature range	−40 to +60 °C
Hub height	30 m
Type	3 Blade Upwind

**Figure 9.** Power curve of the selected wind turbine.

2.6.3. Biogas Generator

A generic biogas generator connected to an AC output is considered for this study. HOMER takes into account the available biogas when sizing the generator. The capital cost, replacement cost, and maintenance costs of a 1-kW biogas generator were set at €1500, €1200, and €0.1/h [15], respectively. The generator lifespan was set at 15,000 h of operation. The minimum load ratio was assumed to be 30% of the capacity. The generator was off for two hours (from 06:00 to 09:00) every weekend for maintenance operations, as shown in Figure 10.

**Figure 10.** The generator schedule.

2.6.4. Pumped-Hydro Storage

The generic 245 kWh pumped-hydro component recently introduced into the HOMER component library was used to model the PHS station in this study. The system can store up to 1000 m³ of water dischargeable over a 12-h period [43], resulting in a discharge flow rate (Q) of 0.0231 m³/s and a

capacity power (P_C) of 20.4 kW. Moreover, the head height of the system (H) was determined at 100 m from the following relationship [17]:

$$P_C = \rho g Q H \eta, \quad (3)$$

where: P_C = power capacity (2,0400 W); ρ = mass density of water (1000 kg/m³); g = acceleration due to gravity (9.8 m/s²); Q = discharge flow rate (0.0231 m³/s); and, η = PHS efficiency when discharging (assumed at 90%).

The costs of pumped-hydro energy storage systems are provided by the Electricity Storage Association and range from €440/kW to €1320/kW [44]. Accordingly, the initial cost of the system can range between €9000 and €27,000. For this study, the initial cost, replacement cost, and O&M cost were taken as €15,000, €10,000, and €300/year. The lifespan of the system was assumed to be 25 years.

2.6.5. Converter

A power converter system is necessary to ensure the continuity of energy flow between the DC and AC electrical components of the system. In this study, a generic system converter comprising an inverter and a rectifier to perform a bidirectional AC-DC conversion was considered. The capital cost, replacement and O&M costs for 1 KW were assumed to be €650, €600, and €0, respectively [15]. The inverter efficiency is considered to be 95%, while the rectifier efficiency is set at 100% to take into account the fact that a rectifier, although required in HOMER implementation, is non-existent in the real system. A converter lifespan of 15 years was considered.

2.7. Simulation and Optimization

2.7.1. The Assessment Criteria

The HOMER's assessment criteria considered for optimal system design is the Total Net Cost (NPC). It is the performance criterion by which all feasible system configurations are ranked in the optimization results. The NPC is the sum of all discounted values of costs and revenues related to the system. In the present case, the costs included the upfront costs, replacement costs, operating costs, and fuel cost, while the revenues involved salvage values of the system components. The NPC of an HRES is expressed, as follows [38]:

$$NPC = \frac{C_{ann,tot}}{CRF(d, N)}, \quad (4)$$

where $C_{ann,tot}$ = total annualized cost of the system, CRF = Capital recovery factor, N = project lifespan, and d = discount rate.

The total annualized cost of the system is given as:

$$C_{ann,tot} = C_{ann,cap} + C_{ann,rep} + C_{ann,O\&M} + C_{ann,fuel} - R_{ann,salv} \quad (5)$$

where $C_{ann,cap}$, $C_{ann,rep}$, and $C_{ann,O\&M}$ are, respectively, the annualized capital, replacement, and maintenance costs of all components of the system; $C_{ann,fuel}$ is the annualized cost of fuels used to feed the power generators, and $R_{ann,salv}$ represents the annualized total savage value of all system components. A Capital Recovery Factor (CRF) converts a present value into a uniform annual cash flow series over the project lifespan (N) at a specified discount rate (d). CRF formula is given as:

$$CRF = \frac{d(1+d)^N}{(1+d)^N - 1}. \quad (6)$$

In this study, the life of the project was set at 20 years. The discount rate is calculated on the basis of the following equation [15]:

$$d = \frac{i - f}{1 + f}, \quad (7)$$

where f is the annual inflation and i the nominal interest rate. The annual inflation rate and nominal interest rate were considered at 3% and 8%, respectively.

Besides the NPC, HOMER also calculates the levelized cost of energy (COE). This is the average cost of production by the system of one kWh of electricity. COE is expressed as the ratio of the total annualized cost of the system to the total annual useful electricity output of the system. The formula of COE is given as [34]:

$$\text{COE} = \frac{C_{ann,tot} - C_{boiler} \cdot H_{thermal}}{E_{served}} \quad (8)$$

where $C_{ann,tot}$ = the total annualized cost of the system (€/year), C_{boiler} = boiler marginal cost (€/kWh), H_{served} = total thermal load served (kWh/year), and E_{served} = total electrical load served (kWh/year). In this study, thermal load is not served, hence $H_{served} = 0$.

2.7.2. Dispatch Strategy

A dispatch strategy is a set of rules governing the operation of the generator(s) and the storage device(s). HOMER software can model two dispatch strategies: load following (LF) and cycle charging (CC) [38]. Under the load following strategy, whenever a generator is activated, it only produces the power that is needed to meet the demand; while under the cycle charging strategy, each time a generator is turned on, it runs at full capacity, the surplus power being stored by the power storage device. Both LF and CC strategies were considered in this study.

2.7.3. Optimization Variables and Search Space

An optimization variable, also referred to as decision variable, is a variable that can be controlled by the system designer and for which HOMER can take into account several possible values in its optimization process. Table 8 displays the optimization variables involved in this study and related values to each one. They include the size of the PV array (seven values), the number of wind turbines (10 values), the number of pumped hydro storage stations (six values), the size of the biogas generator (eight values), and the size of the bidirectional converter (nine values). The search space is the set of all possible system configurations in which HOMER searches for the optimal solution. For this study, each combination of the five optimizations variables was simulated for each of the two dispatch strategies considered (LF and CC). The number of configurations simulated by the HOMER software was therefore $7 \times 10 \times 6 \times 8 \times 9 \times 2 = 60,480$ configurations.

Table 8. Optimization variables of the study model.

Optimization variable	PV Array Size (kW)	Number of WT	Number of Pumped Hydro Storage (PHS) (number)	Biogas Generator Size (kW)	Converter Capacity (kW)
Maximum	98.1	9	5	17.5	80
Minimum	0	0	0	0	0
Step	16.35	1	1	2.5	10

2.7.4. Constraints

Constraints are conditions that system configurations must satisfy. A configuration that does not meet one of the specified constraints is considered an unfeasible configuration and is not ranked by HOMER after the simulation and optimization process. Two types of constraints are considered in the present case study:

- The constraint that is related to the capacity shortage is defined by the maximum annual capacity shortage, which was set at 5% in this study. This means that HOMER discarded any system that did not meet at least 95% of the annual electrical load plus the operating reserve.
- Constraints related to the operating reserve are those that impose excess operating capacity to ensure the reliability of the system in the event of a sudden increase in load or a reduction in

renewable energy production. HOMER defines the required operating reserve using four inputs, two of which are as a percentage of the variability of the electricity load: load in current time step and annual peak load; and two as a percentage of renewable energy production: solar power output and wind power output. In this case study, the operating reserve percentages that are associated with the load in current time step, annual peak load, solar power output, and wind power output were set at 10%, 15%, 20%, and 50%, respectively.

2.8. Sensitivity Analysis

Sensitivity analysis aims at dealing with uncertainty by investigating the effects of changes in specific parameters on the performance of the system. A parameter is any HOMER's numerical input data that is not a decision variable. Parameters that are involved in a sensitivity analysis are sometimes referred to as sensitivity variables. For each sensitivity variable, a range of values, sensitivity values, is entered into HOMER by the designer. The sensitivity variables considered in this study included wind speed, solar radiation, biomass price, biomass availability, and maximum capacity shortage. All of these sensitivity variables and their associated values are listed in Table 9.

Table 9. Sensitivity variables and associated values.

Sensitivity Variable	Values
Wind speed (m/s)	3.5, 4.95, 8
Solar radiation (kWh/m ² /day)	3.8, 5.82, 7, 8
Capital cost multiplier of PV	0.5, 1, 1.5, 2
Capital cost multiplier of PHS	0.5, 1, 1.5, 2
Biomass price (€/t)	0, 0.2, 0.4, 0.6
Biomass availability (t/day)	0.2, 2.2, 4.5, 7, 9.5
Maximum capacity shortage (%)	0, 2.5, 5, 7.5, 10, 12.5

For speeding up purposes, the sensitivity analyzes were performed sequentially, instead of running them all at the same time. Sensitivity analysis of wind speed and solar radiation was first performed to account for the wide variability in the availability of these two resources, and hence better understand the performance of the proposed system across the sub-Saharan region. The sensitivity analysis of the availability and cost of biomass resources was then conducted to determine the viability of their transport or purchase in the event of unavailability or insufficient production at the site. This was followed by the sensibility analysis of the capital costs of PV and PHS, using cost multipliers, with three objectives: (1) to understand how PV-based HRESs are promising in taking up rural electrification challenges in SSA; (2) to assess the impact of the adoption of PV investment subsidies on the viability of HRESs; and, (3) to evaluate the effect of change in pumped hydro investment cost due site morphology. Finally, the sensitivity analysis of the maximum capacity shortage was run to better manage the trade-off between the reliability and cost of the proposed system.

2.9. The grid Extension

As mentioned above, grid extension is one of the most common rural electrification solutions in sub-Saharan Africa. In this study, it was considered to be an alternative to the proposed off-grid hybrid system. HOMER software when compared both methods by calculating the break-even grid extension distance (BGED) which is the distance from the grid to which the NPCs of the grid extension and the optimized off-grid system are equal. Beyond this distance, the off-grid system is preferable, while closer to the grid, the grid extension is the best solution. The required input parameters for performing the BGED calculation in HOMER are the capital cost per km, annual O&M cost per km, and the grid power price.

The capital cost per km and the O&M cost of the grid extension were, respectively, estimated at €10,000/km and €200/year/km in [18,45]. Given inflation, they were taken at €14,000/km and €300/year/km in this analysis. The average price of electricity from the grid in Cameroon is 0.1 €/kWh.

3. Results

The results of the analyses described above are presented in this section. The optimization results are first analyzed, followed by the description of the sensitivity analyses outcomes.

3.1. Optimization Results

The results of HOMER simulation and optimization processes showed that among the 60,480 system configurations of the HOMER search space, only 11,560 were feasible and classified according to the system architecture in five categories, namely: category 1 (PV/Biogas/PHS), category 2 (PV/Wind/Biogas/PHS), category 3 (PV/PHS), category 4 (PV/Wind/PHS), and category 5 (Wind/Biogas/PHS). The details of the components, as well as the technical and economic specifications of the best hybrid system in each category, are presented in Table 10. The best hybrid system in Category 1, which was the overall optimal hybrid system, was made up of an 81.8 kW PV array, a 15 kW biogas generator, two 245 kWh pumped hydro storage stations, and a 40 kW bi-directional converter with a dispatch strategy of load following. No wind turbine is included in that configuration. Its cost of energy (COE) and total net present cost (NPC) were €0.256/kWh and €370,426 respectively.

The breakdown by component and cost type of this NPC, as presented in Figure 11, shows that it was 87% dominated by the total capital cost of the system. The PV array was the most important component in terms of costs and accounted for 76% of the total capital cost and 66% of the NPC of the system. During the life of the project, only the biogas generator and system converter were replaced for a total replacement cost of €28,066. For this configuration, the total annual electricity production was 159,840 kWh/year, 89% dominated by the production of photovoltaic panels.

Figure 12, which displays the monthly distribution of electrical generation shows that the power generation from biogas generator was higher during the dry season (October to April) than the rainy season. The excess energy and the unmet load for that configuration were, respectively, 13,670 kWh/year and 1972 kWh/year, i.e., 8.6% and 1.6% of total production. An excess electricity is an unused and dumped power once the electrical load demand is met and the upper reservoir of the PHS station is full, while an unmet load is a load that cannot be met due to a gap between the total electrical demand and the total electrical generating capacity. The system's capacity shortage was 6071 kWh/year, i.e., 4.8% of the demand load, which is less than the maximum shortage capacity of 5%, specified as a constraint.

The PV array output throughout the year, shown in Figure 13, reveals that the PV power production took place between 06:00 and 18:00 and it was more likely to reach its maximum (75.7 kW) between 10:00 and 14:00. Furthermore, the total annual PV electrical production was 141,046 kWh/year, which corresponded to a capacity factor of the system of 19.7%.

Figure 14 shows the performance of the biogas generator throughout the year. During the rainy season (May to September), it was more likely that the generator was switched on between 18:00 and midnight, while, during the dry season (October to April), it was from 14:00 to midnight. For both seasons, the biogas generator was likely to deliver its maximal electrical output (14.8 kW) between 18:00 and 00:00. The annual power production from biogas generator was 17,794 kWh/year, representing a capacity factor of the system of 13.5%.

Table 10. Optimization results.

Specification Category	Specification	Unit	Best Hybrid System Per Category				
			Category 1	Category 2	Category 3	Category 4	Category 5
System architecture	PV array 5SPR-E20	kW	81.8	65.4	98.1	81.8	0
	Wind turbine (XL10R)	Number	0	1	0	1	8
	Biogas gen.	kW	15	15	0	0	12.5
	Pumped Hydro (PH 245)	Number	2	2	3	3	4
	Converter	kW	40	40	50	50	70
	Dispatch strategy	LF or CC	LF	LF	CC	CC	CC
Cost	LCOE	€/kWh	0.256	0.260	0.261	0.265	0.417
	NPC	€	370,426	375,945	379,257	383,757	598,368
	Total O&M cost	€/year	4031	4425	644	950	6400
	Total capital cost	€	323,750	324,700	371,800	372,750	524,250
Power production	PV array	kWh/year	141,046	112,837	169,255	141,046	0
	Wind turbine	kWh/year	0	19,031	0	19,031	152,249
	Biogas Generator	kWh/year	17,794	18,508	0	0	17,323
	Total electricity production	kWh/year	158,840	150,376	169,255	160,077	169,572
	Primary load consumption	kWh/year	125,056	124,916	125,225	124,888	123,901
	Capacity shortage	kWh/year (%)	6.071 (4.8)	6430 (5)	4756 (3.7)	6269 (4.9)	6377 (5)
	Unmet load	kWh/year (%)	1972 (1.6)	2112 (1.7)	1503 (1.2)	2140 (1.7)	3127 (2.4)
	Excess electricity	kWh/year (%)	13,670 (8.6)	7158 (4.8)	19,249 (11.4)	12,532 (7.8)	27,693 (15.9)
Capacity factor	PV array 5SPR-E20	%	19.7	19.7	19.7	19.7	0
	Wind turbine (XL10R)	%	0	21.7	0	21.7	21.7
	Biogas gen.	%	13.5	14.1	0	0	18.8

The results of our model also show that the PHS total input and output power were respectively 78,501 kWh/year and 64,050 kWh/year, the difference resulting from the system losses (14,968 kWh/year) and the depletion of storage (508 kWh/year). This value of losses correspond to a conversion efficiency of 20%, which is in the 65%–80% range of round-trip energy efficiency of pumped-hydro storage systems [24]. Losses in pumped-hydro storage systems are mainly made up of pipe friction losses and pump/turbine unit losses [46].

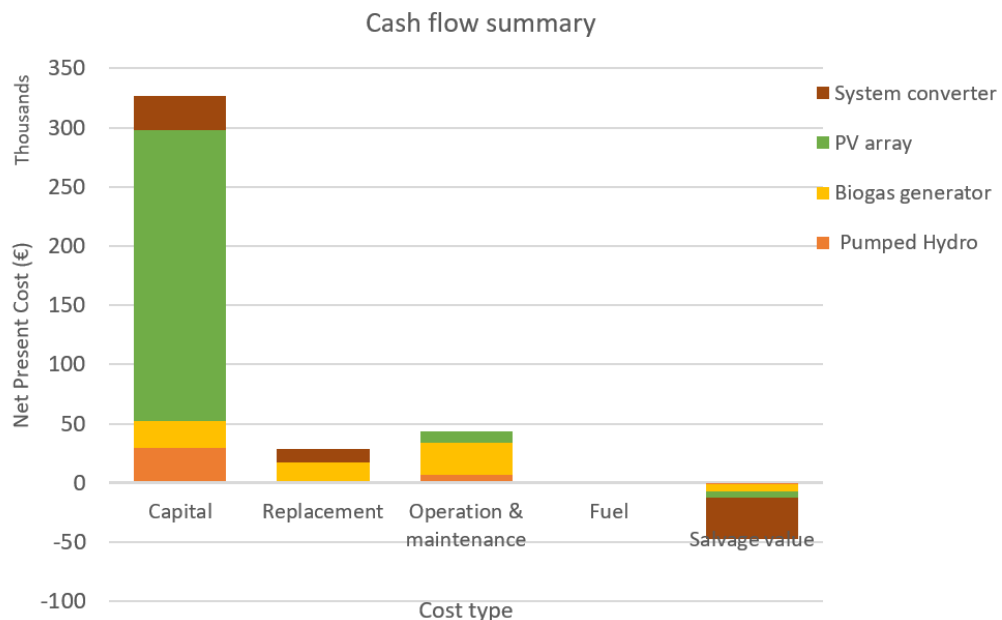


Figure 11. Cash flow summary based on the optimised architecture.

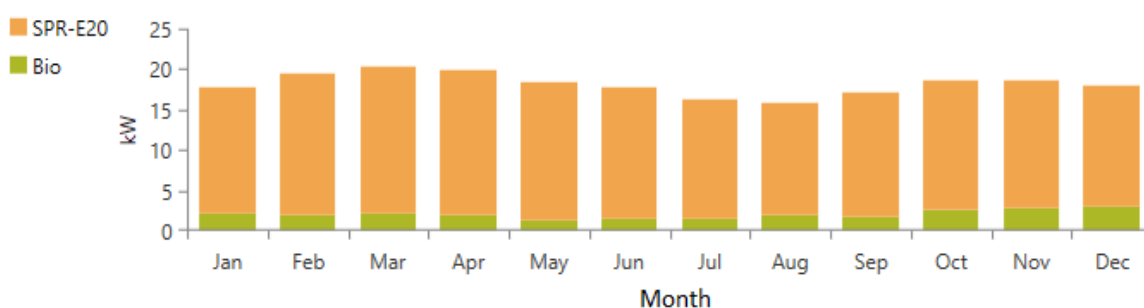


Figure 12. Monthly average electrical output from the optimal configuration system.

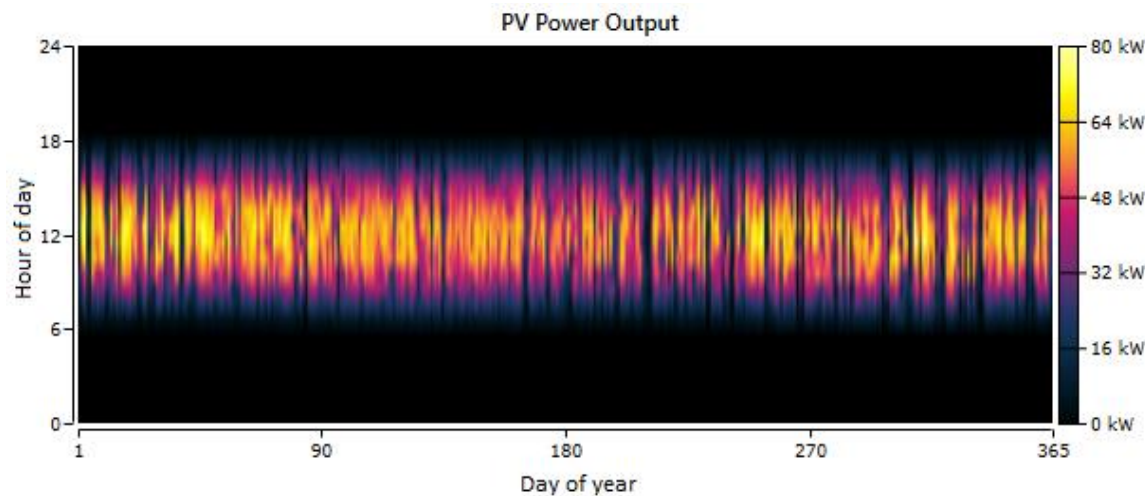


Figure 13. The PV array output.

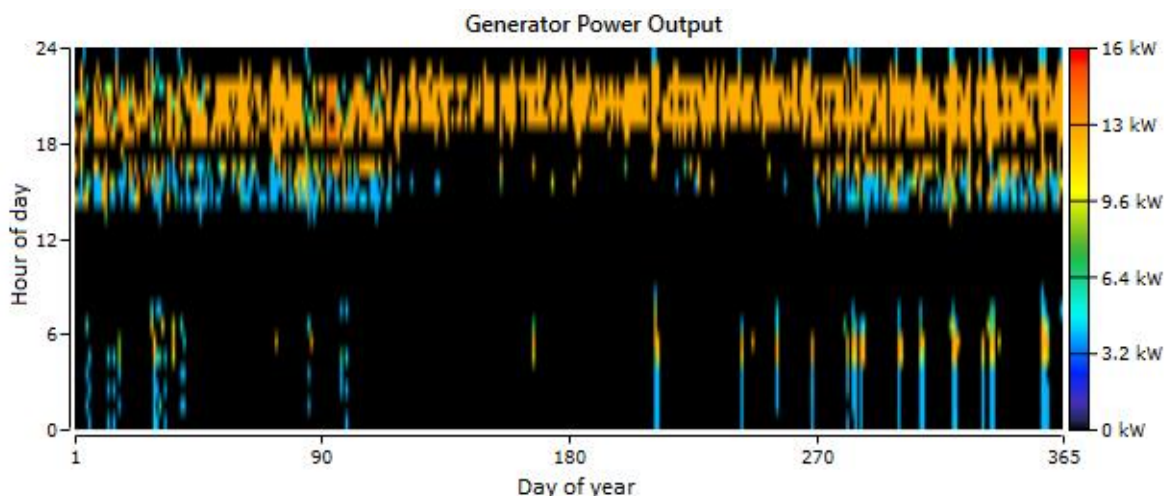


Figure 14. Biogas generator output.

Figure 15, which displays the state of charge of the pumped hydro storage station of the present case, shows that the upper reservoir was relatively more filled during the rainy season than the dry season. This was due to the relatively higher demand for electrical energy during the dry season than during the rainy season, which implied a higher probability of occurrence of unmet load during the dry season.

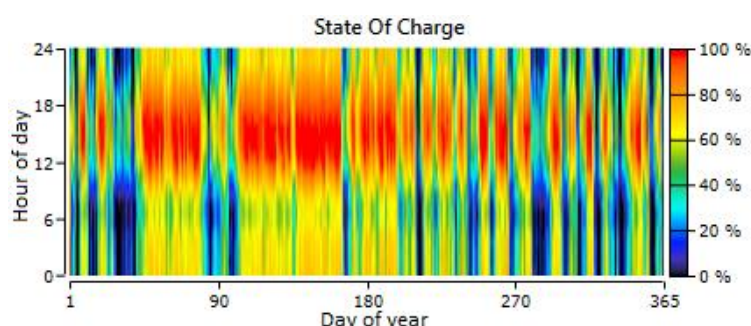


Figure 15. State of charge of the Pumped-hydro storage station.

Figure 16 shows the operating schedules and energy flow of optimized system components over a 72-hour period (29, 30 and 31 December) during the dry season. During the day (8:00–17:00) due to the intense sunlight, the PV output was high and intended to meet the load demand and charge the PHS station. From 8:00 to 12:00, the pumped hydro charge power was likely to peak due to low load demand, and excess power production was likely to occur, as was the case on 29 December. From 12:00 to 18:00, the PV array output might become insufficient to meet the demand load and charge the PHS station, requiring the activation of the biogas generator to fill the gap, as was the case on 29, 30 and 31 December. During the night and early in the morning (17:00–8:00), because of the absence of sunshine, the PV array output was zero so that the demand for electrical energy was mainly satisfied by the power output from the PHS station. However, from 18:00 to 0:00, after peaking, this power became insufficient to cover the load demand, requiring the activation of biogas generator to fill the gap. The latter might in turn also peak without filling the gap for which it had been activated, resulting in an unmet load, as was the case on 30 and 31 December. From 0:00 to 8:00, the low load demand was exclusively satisfied by the PHS output.

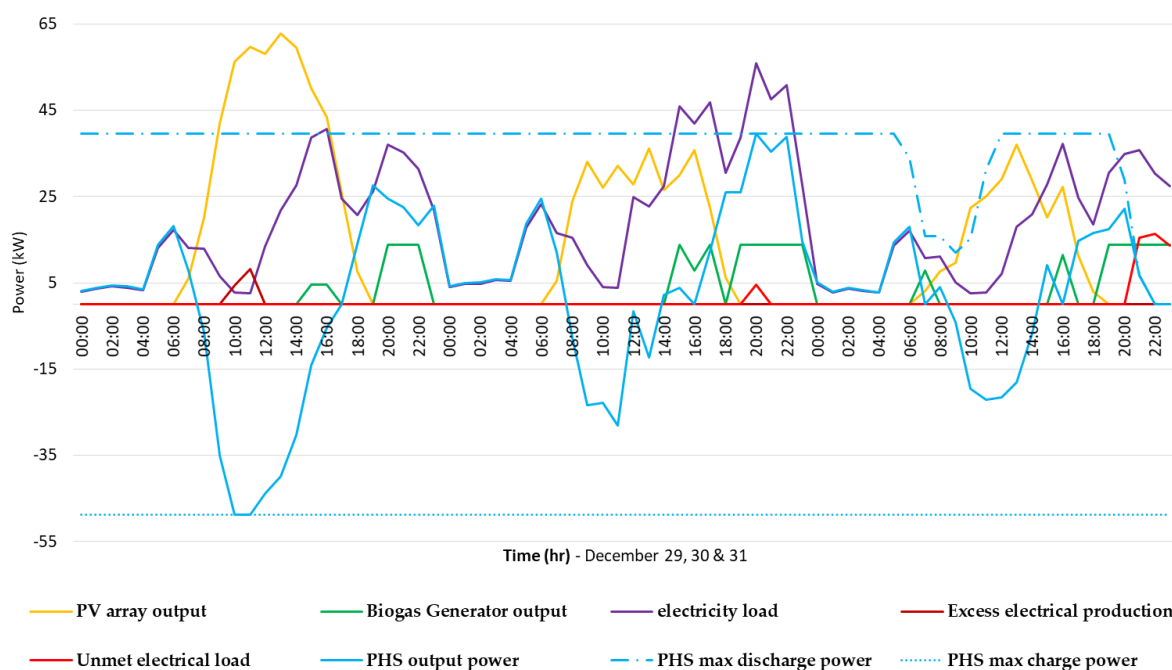


Figure 16. Operations schedules and energy flow of the system components over a 72-hour period.

Figure 17 shows the result of the comparison between the NPCs of the autonomous system designed and the grid extension for the purpose of electrification of Djoundé. This indicates a break-even grid extension distance of 12.78 km, which led to the conclusion that the system designed was the better solution for Djoundé's electrification, with the nearest power transformer being located in Mora, 18 km away.

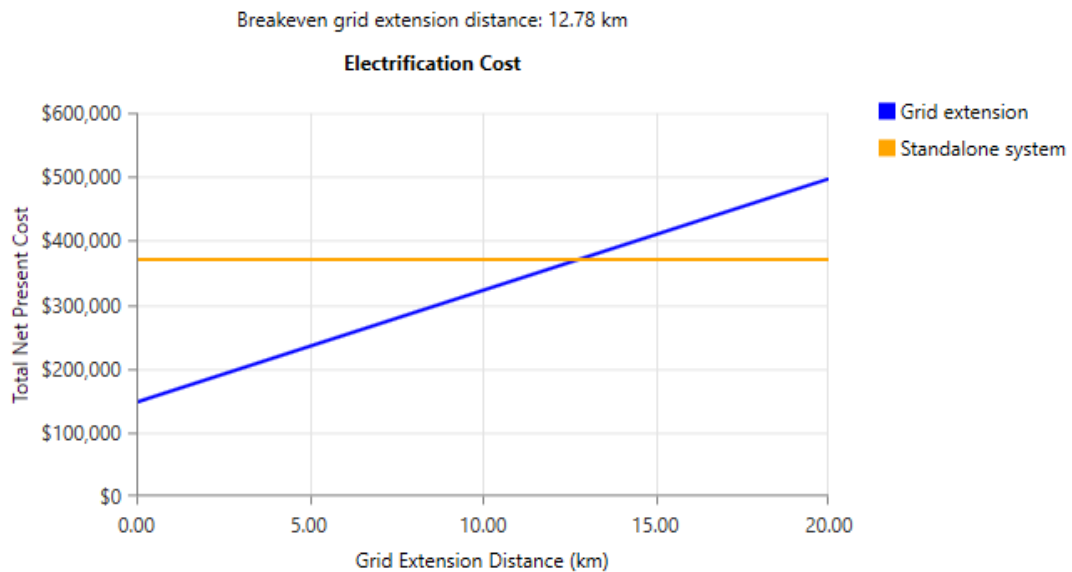


Figure 17. Cost of electrification options of Djoundé.

3.2. Sensitivity Results

The sensitivity result for wind speed and solar radiation is presented in Figure 18. It shows that, for low wind speed values, the optimal system type would be PV/Biogas/PHS; hence, the COE and NPC of the system would not be sensitive to wind speed variation, as no wind turbine would be part of the system. However, for each solar radiation value, increasing, the wind speed would reach a threshold value above which the optimal system type would be PV/Wind/Biogas/PHS. By increasing further above that threshold value, the wind speed would reach another threshold value, above which the optimal system type would be Wind/Biogas/PHS. The higher the solar radiation, the higher the two wind speed threshold values mentioned above. For all wind speed values that are below 6 m/s, the PV array would be part of the optimal-system components, and the higher the solar radiation, the lower the NPC and COE. For very high wind speed values, the PV array would not be part of the system; hence the system performances were not sensitive to variations in solar radiation. Therefore, if only the changes in solar radiation and wind speed were taken into account, the optimal system type would be PV/Biogas/PHS and it would have COEs greater than €0.3/kWh in parts of SSA such as Gabon, Equatorial Guinea, Southern Cameroon, Southern Nigeria and Congo, which experience average solar radiations below 5 kWh/day/m², and wind speed less than 4.5 m/s [47,48]. The optimal system type would remain PV/Biogas/PHS, but COEs would be reduced to less than 2.5 €/kWh in some such places as Northern Chad and Northern Niger. The wind turbines would be part of the optimal system in the places with higher wind speed, which would help to reduce the COE up to 2 €/kWh in the regions such as the East African and South African coasts that experience wind speed greater than 7 m/s.

Figure 19 presents the result of the sensitivity analysis of the capital costs of PV and PHS systems. The capital cost of PHS showed a less potential impact on the optimal system type and COE. For example, doubling it would not change the optimal system type and it would increase its COE by only 8%. On the other hand, for a 50% reduction in capital cost of PV, the optimal system would change from PV/Biogas/PHS type to PV/PHS type, and its COE would decrease by 37%. For a 50% increase in the PV capital cost, wind turbines would be integrated into the optimal system of which the COE would increase by 29%. Therefore, PV-based HRESs are promising for addressing the challenges of rural electrification in sub-Saharan Africa Given that PV capital cost is expected to decrease by 50% by 2040 [49]. The result of this analysis also highlighted the relevance of government subsidies to the investment costs of photovoltaic technology for PV-HRESs to be viable. On the other hand, the

morphology of the site, although having a significant impact on the investment cost of PHS systems, does not affect the viability of the latter as an energy storage device for HRESs in the region.

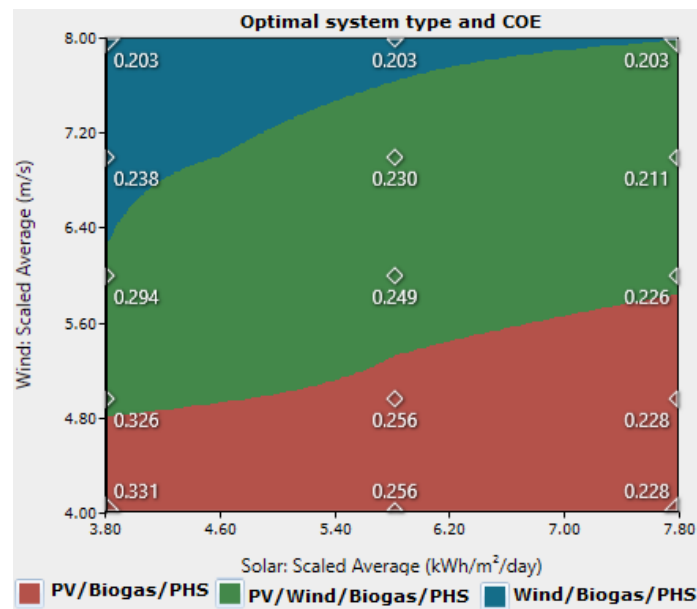


Figure 18. Result of sensitivity analysis of wind speed and solar radiation.

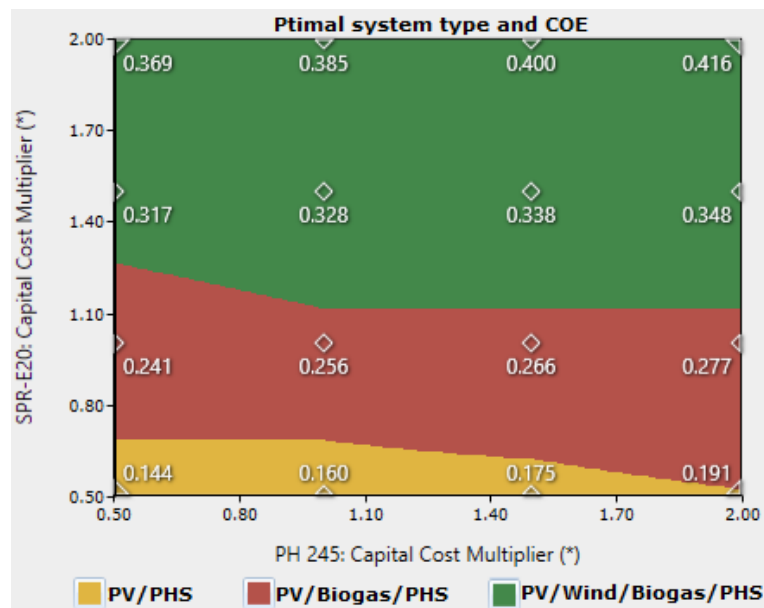


Figure 19. Sensitivity analysis result of PV and PHS capital costs.

Figure 20 presents the result of the sensitivity analysis of the availability and cost of biomass resources. It shows that in the case of deficient biomass resource production, the use of the biogas generator as the backup engine would be infeasible. However, increased availability above the calculated value would not have a significant impact on the system performance. For example, doubling the value of the base scenario would result in only a 0.2% decrease in the system's COE. On the other hand, the result shows that, if the biomass availability value of the base scenario is considered, the biogas generator would no longer be viable if the biomass price was greater than €0.13/t. Thus, in

the event of unavailability at the site, the transport or the purchase of biomass resource would not be viable. However, that unavailability would only increase the COE by 2%.

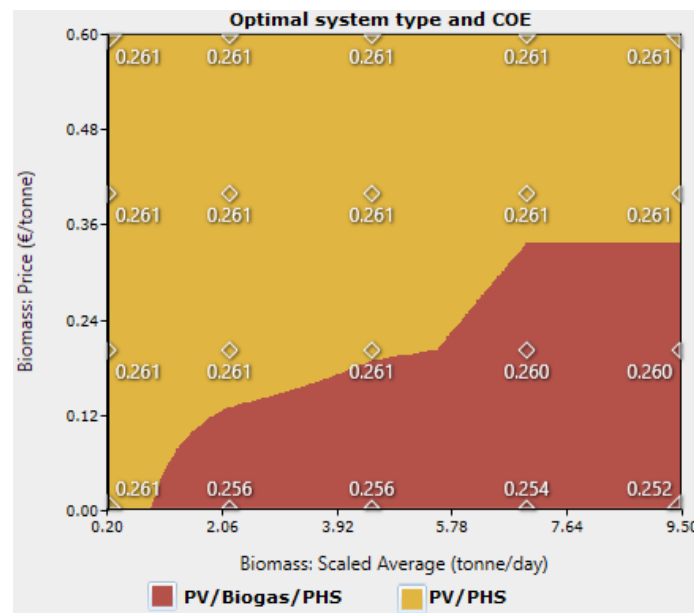


Figure 20. Sensitivity analysis result of the price and availability of biomass.

The result of the sensitivity analysis of maximum capacity shortage is illustrated in Figure 21. It shows that an improvement of the reliability of the system by lowering the maximum annual capacity shortage from 5% to 2.5% would result in NPC and COE increases of only 0.6% and 0.4%, respectively, while an improvement to 0% would result in increases of 9% and 7%, respectively. On the other hand, the degradation of the system reliability by setting its maximum annual capacity shortage at 10% would decrease its NPC and COE by 4% and 3%, respectively. This result reveals that the system could achieve better reliability without substantially increasing the COE.

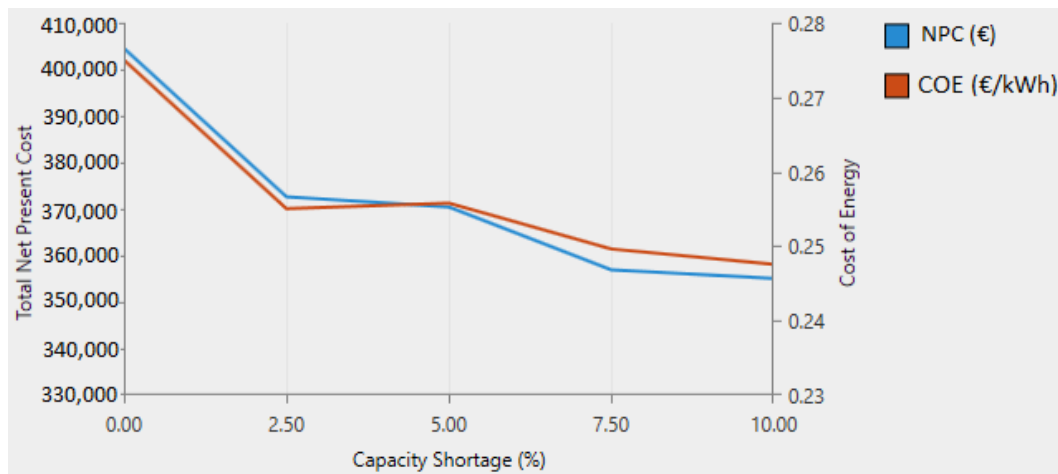


Figure 21. Sensitivity analysis result of the maximum capacity shortage.

4. Discussion

The results of the analyses that are presented above clearly show that the proposed system could help to meet the demand for electricity in a remote village at a lower COE than in any of the previous cases in sub-Saharan Africa cited in the literature review of this article [11,12,15,18]. Each of these cases

had a battery system as an energy storage device, which demonstrates to the point that PHS-based hybrid renewable energy systems are technically and economically better than battery-based systems, and confirms the hypothesis defined in the introductory part. Moreover, unlike previous studies, the analysis of the system was preceded by a thorough assessment of electricity demand taking into account all electricity consumption sectors, including agriculture, the primary sector of employment in rural areas of SSA. This implies a more realistic and reliable assessment of load demand, which advances the literature on HRES applications in sub-Saharan Africa.

At the global level, the novelty of this study lies on two points. First, the authors have successfully modelled, simulated, and optimized a PHS based HRES using the 245 kWh PHS component recently introduced by HOMER. The roundtrip efficiency of the modelled PHS system was within the typical value range of real production environments. Other authors have attempted to solve the same problem, namely Ma et al. [17], who developed mathematical models to model and simulate dozen feasible configurations a PHS-based PV/Wind hybrid system to meet the electricity demand of a remote island in Hong Kong. The main limitation of the study by Ma et al. is that the designed models were not able to achieve the optimization of the system. To fill the absence of a PHS component in the HOMER library, Canales and Beluco [50] proposed a method of modelling a pumped-hydro energy storage system with HOMER by making certain adjustments on a battery component for that it represents a PHS system. This approach was then implemented in [51] to model, simulate, and optimize a PHS based energy system to meet the electrical load of a village in South Africa. Although Canales and Beluco's proposed approach allows for optimizing PHS based on HRESs, it has the disadvantage of requiring prior adjustments to specific HOMER components. Also, the introduction of the 245 kWh PHS component in HOMER library has reduced its usefulness. Besides, models developed by Kusakana [21], cited and described in the introductory part of this paper presents less relevance in the context of SSA as cost reduction was not the primary objective of the analysis. When compared to the three preceding approaches, the method devised in this study has the advantage of providing simple modelling, simulation, and cost-based optimization of PHS based HRESs using HOMER software.

The second novelty of this paper lies with providing possible interpretations of sensibility analysis results other than those that highlight the effect of the change in key parameters on the system performance. Among the studies reviewed in this paper, those that performed a sensitivity analysis [13–15,19,20] failed in broadening the interpretation of their analysis results. Unlike previous those studies, this article was able to interpret the result of the sensitivity of wind speed and solar radiation to provide insight into the performance of the proposed system throughout the SSA region. Such information is essential for determining the level of a renewable energy policy to improve the viability of the system in a particular location. Then, the result of the sensitivity analysis of capital costs of PV and PHS systems provides insight into the potential effect of the government's PV capital cost subsidies, as well as the promising prospects of PV based HRESs giving the upcoming decrease in PV capital costs. Such information is essential for the government in designing appropriate policies for microgrid technology. Finally, the sensitivity analysis of the availability and cost of biomass resources provided an overview of the relevance of transportation or purchase of these resources. This information is essential in a resource-limited environment. Indeed, Biomass resources may not be available at the site or may be sought for other uses, such as cooking, soil fertility, or agricultural traction [52]. For illustrative purposes: the biomass available in the baseline scenario could produce 78 m³ of biogas per day, enough to meet the daily cooking needs of nearly 344 people in rural areas of sub-Saharan Africa, considering that the daily amount of biogas that is required for cooking per person in rural areas is 0.227 m³/day [53].

Primary beneficiaries of the implementation of this research will be the local populations of Djoundé who will benefit from the project in three points. First, the provision of electricity to the agricultural sector will help solve the crucial problem of poor agricultural performance in the area through the use of electrical machinery in agricultural production, full mechanization, and processing of agricultural products. Indeed, the lack of energy has been reported as the leading cause of the

low productivity of the agricultural sector in sub-Saharan Africa, where only 2% of final electricity consumption is devoted to agriculture, as compared to 18% in India [2]. Second, the project is expected to promote the development of small-scale industry and commerce, which will help increase productivity and lead to job creation and poverty reduction [3,5]. Finally, the implementation of the project will contribute to improving the quality of life, health outcomes, gender equality, education, and ending migration and deforestation [4,6].

The barriers to the implementation of the research envisioned in this paper are: high investment costs; lack of a legal, regulatory and institutional framework; lack of funding; and, unrealistic pricing. Designing appropriate renewable energy incentive policies is a critical step in addressing these challenges and then promoting hybrid renewable energy systems for rural electrification in SSA.

The main tool, HOMER Pro, used to perform this research is a Windows application requiring Windows 7, 8, 8.1, or higher.

The originality of this study can be emphasized in three points, namely: (1) the use of HOMER software to model and simulate a pumped-hydro energy storage based HRES; (2) consideration of the agricultural sector and the seasonal variation in the assessment of electricity demand of a rural area of sub-Saharan Africa; and, (3) broadening sensitivity analysis applications to address practical issues that are related to HRESs.

Additional studies are needed to address the limitations of this study, the main ones being: (1) the failure to take into account the increase in energy demand over time due to population growth and technological development; (2) the non-consideration of social and environmental factors in the selection of the best system configuration; and, (3) the failure to account for the losses imposed on the surplus power of the PV array and the wind turbine due to the HOMER modelling of the PHS system as a battery connected to the DC bus.

5. Conclusions

In response to the challenges of rural electrification in sub-Saharan Africa, a 100% renewable hydro-pumped off-grid hybrid energy system, consisting of wind turbines, PV array, and a biogas generator, has been proposed to meet the demand for electricity in Djoundé, a remote village on northern Cameroon. By designing and applying an original approach, we achieved the modeling, simulation, and optimization of the proposed system. The results of the study highlighted the cost-effectiveness and environmental benefits of the proposed system when compared to previous cases in sub-Saharan Africa. Therefore, PHS-based HRESs can be part of solution in achieving “access to affordable, reliable and modern energy for all by 2030”, in line with the Millennium Development Goals (MDGs) for energy. Therefore, sub-Saharan African countries are called upon to develop appropriate policies to address hindering factors to the implementation of HRESs.

Author Contributions: Conceptualization, N.Y., O.H. and L.M.; Methodology, N.Y., B.N. and O.H.; Modelling, N.Y.; Validation, O.H., L.M. and B.N.; Formal Analysis, N.Y., O.H. and L.M.; Investigation, L.M. and B.N.; Writing-Original Draft Preparation, N.Y.; Writing-Review & Editing, L.M., O.H., B.N. and J.N.; Supervision, J.N.

Funding: No external funding was provided for this research.

Conflicts of Interest: The authors declare no conflict of interest.

References

1. Riva, F.; Ahlborg, H.; Hartvigsson, E.; Pachauri, S.; Colombo, E. Electricity access and rural development: Review of complex socio-economic dynamics and causal diagrams for more appropriate energy modelling. *Energy Sustain. Dev.* **2018**, *43*, 203–223. [[CrossRef](#)]
2. World Energy Outlook Special Report. Energy Access Outlook 2017: From Poverty to Prosperity. Available online: https://www.iea.org/publications/freepublications/publication/WEO2017SpecialReport_EnergyAccessOutlook.pdf (accessed on 10 September 2018).
3. Adams, S.; Klobodu, E.K.M.; Opoku, E.E.O. Energy consumption, political regime and economic growth in sub-Saharan Africa. *Energy Policy* **2016**, *96*, 36–44. [[CrossRef](#)]

4. Trotter, P.A. Rural electrification, electrification inequality and democratic institutions in sub-Saharan Africa. *Energy Sustain. Dev.* **2016**, *34*, 111–129. [[CrossRef](#)]
5. Feder, G.; Savastano, S. Modern agricultural technology adoption in sub-Saharan Africa: A four-country analysis. In *Agriculture and Rural Development in a Globalizing World*; Routledge: Abingdon-on-Thames, UK, 2017; pp. 11–25.
6. Orlando, M.B.; Janik, V.L.; Vaidya, P.; Angelou, N.; Zumbyte, I.; Adams, N. Getting to Gender Equality in Energy Infrastructure: Lessons from Electricity Generation, Transmission, and Distribution Projects. 2018. Available online: <http://documents.worldbank.org/curated/en/930771499888717016/pdf/117350-ESMAP-P147443-PUBLIC-getting-to-gender-equality.pdf> (accessed on 12 August 2018).
7. Dagnachew, A.G.; Lucas, P.L.; Hof, A.F.; Gernaat, D.E.; de Boer, H.-S.; van Vuuren, D.P. The role of decentralized systems in providing universal electricity access in Sub-Saharan Africa—A model-based approach. *Energy* **2017**, *139*, 184–195. [[CrossRef](#)]
8. McCright, A.M.; Dunlap, R.E. The politicization of climate change and polarization in the American public's views of global warming, 2001–2010. *Sociol. Q.* **2011**, *52*, 155–194. [[CrossRef](#)]
9. Lauber, V.; Jacobsson, S. The politics and economics of constructing, contesting and restricting socio-political space for renewables—The German Renewable Energy Act. *Environ. Innov. Soc. Transit.* **2016**, *18*, 147–163. [[CrossRef](#)]
10. Sinha, S.; Chandel, S. Review of software tools for hybrid renewable energy systems. *Renew. Sustain. Energy Rev.* **2014**, *32*, 192–205. [[CrossRef](#)]
11. Nfah, E.; Ngundam, J. Feasibility of pico-hydro and photovoltaic hybrid power systems for remote villages in Cameroon. *Renew. Energy* **2009**, *34*, 1445–1450. [[CrossRef](#)]
12. Adaramola, M.S.; Agelin-Chaab, M.; Paul, S.S. Analysis of hybrid energy systems for application in southern Ghana. *Energy Convers. Manag.* **2014**, *88*, 284–295. [[CrossRef](#)]
13. Halabi, L.M.; Mekhilef, S.; Olatomiwa, L.; Hazelton, J. Performance analysis of hybrid PV/diesel/battery system using HOMER: A case study Sabah, Malaysia. *Energy Convers. Manag.* **2017**, *144*, 322–339. [[CrossRef](#)]
14. Singh, S.; Singh, M.; Kaushik, S.C. Feasibility study of an islanded microgrid in rural area consisting of PV, wind, biomass and battery energy storage system. *Energy Convers. Manag.* **2016**, *128*, 178–190. [[CrossRef](#)]
15. Sigarchian, S.G.; Paleta, R.; Malmquist, A.; Pina, A. Feasibility study of using a biogas engine as backup in a decentralized hybrid (PV/wind/battery) power generation system—Case study Kenya. *Energy* **2015**, *90*, 1830–1841. [[CrossRef](#)]
16. Baghdadi, F.; Mohammedi, K.; Diaf, S.; Behar, O. Feasibility study and energy conversion analysis of stand-alone hybrid renewable energy system. *Energy Convers. Manag.* **2015**, *105*, 471–479. [[CrossRef](#)]
17. Ma, T.; Yang, H.; Lu, L.; Peng, J. Technical feasibility study on a standalone hybrid solar-wind system with pumped hydro storage for a remote island in Hong Kong. *Renew. Energy* **2014**, *69*, 7–15. [[CrossRef](#)]
18. Kenfack, J.; Neirac, F.P.; Tatielse, T.T.; Mayer, D.; Fogue, M.; Lejeune, A. Microhydro-PV-hybrid system: Sizing a small hydro-PV-hybrid system for rural electrification in developing countries. *Renew. Energy* **2009**, *34*, 2259–2263. [[CrossRef](#)]
19. Singh, S.S.; Fernandez, E. Modeling, size optimization and sensitivity analysis of a remote hybrid renewable energy system. *Energy* **2018**, *143*, 719–731. [[CrossRef](#)]
20. Ahmad, J.; Imran, M.; Khalid, A.; Iqbal, W.; Ashraf, S.R.; Adnan, M.; Ali, S.F.; Khokhar, K.S. Techno economic analysis of a wind-photovoltaic-biomass hybrid renewable energy system for rural electrification: A case study of Kallar Kahar. *Energy* **2018**, *148*, 208–234. [[CrossRef](#)]
21. Kusakana, K. Optimization of the daily operation of a hydrokinetic–diesel hybrid system with pumped hydro storage. *Energy Convers. Manag.* **2015**, *106*, 901–910. [[CrossRef](#)]
22. Sawle, Y.; Gupta, S.; Bohre, A.K. Socio-techno-economic design of hybrid renewable energy system using optimization techniques. *Renew. Energy* **2018**, *119*, 459–472. [[CrossRef](#)]
23. Aoudji, A.K.; Kindzoun, P.; Adegbidi, A.; Ganglo, J.C. Land Access and Household Food Security in Kpomassè District, Southern Benin: A Few Lessons for Smallholder Agriculture Interventions. *Sustain. Agric. Res.* **2017**, *6*, 104. [[CrossRef](#)]
24. Luo, X.; Wang, J.; Dooner, M.; Clarke, J. Overview of current development in electrical energy storage technologies and the application potential in power system operation. *Appl. Energy* **2015**, *137*, 511–536. [[CrossRef](#)]

25. Ma, T.; Yang, H.; Lu, L. Feasibility study and economic analysis of pumped hydro storage and battery storage for a renewable energy powered island. *Energy Convers. Manag.* **2014**, *79*, 387–397. [CrossRef]
26. Connolly, D.; Lund, H.; Mathiesen, B.V.; Leahy, M. A review of computer tools for analysing the integration of renewable energy into various energy systems. *Appl. Energy* **2010**, *87*, 1059–1082. [CrossRef]
27. Luna-Rubio, R.; Trejo-Perea, M.; Vargas-Vázquez, D.; Ríos-Moreno, G. Optimal sizing of renewable hybrids energy systems: A review of methodologies. *Sol. Energy* **2012**, *86*, 1077–1088. [CrossRef]
28. Bahramara, S.; Moghaddam, M.P.; Haghifam, M. Optimal planning of hybrid renewable energy systems using HOMER: A review. *Renew. Sustain. Energy Rev.* **2016**, *62*, 609–620. [CrossRef]
29. Shahzad, M.K.; Zahid, A.; ur Rashid, T.; Rehan, M.A.; Ali, M.; Ahmad, M. Techno-economic feasibility analysis of a solar-biomass off grid system for the electrification of remote rural areas in Pakistan using HOMER software. *Renew. Energy* **2017**, *106*, 264–273. [CrossRef]
30. Sen, R.; Bhattacharyya, S.C. Off-grid electricity generation with renewable energy technologies in India: An application of HOMER. *Renew. Energy* **2014**, *62*, 388–398. [CrossRef]
31. Mahlia, T.; Saktisahdan, T.; Jannifar, A.; Hasan, M.; Matseelar, H. A review of available methods and development on energy storage; technology update. *Renew. Sustain. Energy Rev.* **2014**, *33*, 532–545. [CrossRef]
32. NASA Surface Meteorology and Solar Energy. Available online: <https://power.larc.nasa.gov/> (accessed on 10 September 2018).
33. Kidmo, D.K.; Deli, K.; Raidandi, D.; Yamigno, S.D. Wind energy for electricity generation in the far north region of Cameroon. *Energy Procedia* **2016**, *93*, 66–73. [CrossRef]
34. Bhatt, A.; Sharma, M.; Saini, R. Feasibility and sensitivity analysis of an off-grid micro hydro–photovoltaic–biomass and biogas–diesel–battery hybrid energy system for a remote area in Uttarakhand state, India. *Renew. Sustain. Energy Rev.* **2016**, *61*, 53–69. [CrossRef]
35. Hasan, A.M.; Khan, M.F.; Dey, A.; Yaqub, M.; Al Mamun, M.A. Feasibility study on the available renewable sources in the island of Sandwip, Bangladesh for generation of electricity. In Proceedings of the 2nd International Conference on the Developments in Renewable Energy Technology (ICDRET 2012), Dhaka, Bangladesh, 5–7 January 2012.
36. Mandal, S.; Yasmin, H.; Sarker, M.; Beg, M. Prospect of solar-PV/biogas/diesel generator hybrid energy system of an off-grid area in Bangladesh. *AIP Conf. Proc.* **2017**, *1919*. [CrossRef]
37. Wang, L.; Shahbazi, A.; Hanna, M.A. Characterization of corn stover, distiller grains and cattle manure for thermochemical conversion. *Biomass Bioenergy* **2011**, *35*, 171–178. [CrossRef]
38. Lambert, T.; Gilman, P.; Lilienthal, P. Micropower system modeling with HOMER. *Integr. Altern. Sources Energy* **2005**, 379–418.
39. Graham, V.; Hollands, K. A method to generate synthetic hourly solar radiation globally. *Sol. Energy* **1990**, *44*, 333–341. [CrossRef]
40. Distributed Generation Renewable Energy Estimate of Costs. Available online: <Https://www.nrel.gov/analysis/tech-lcoe-re-cost-est.html> (accessed on 10 September 2018).
41. SunPower SPR-E20-327. Available online: <Https://www.energysage.com/panels/SunPower/SPR-E20-327/> (accessed on 10 September 2018).
42. The excel 10 kW Wind Power. Available online: <Availableat:berkeley.com/products/wind-turbines/10kw-berkeley-excel> (accessed on 10 September 2018).
43. Pumped Hydro—Homer Energy. Available online: Https://www.homerenergy.com/products/pro/docs/3.11/pumped_hydro.html (accessed on 10 September 2018).
44. Deane, J.P.; Gallachóir, B.Ó.; McKeogh, E. Techno-economic review of existing and new pumped hydro energy storage plant. *Renew. Sustain. Energy Rev.* **2010**, *14*, 1293–1302. [CrossRef]
45. Zachary, O.; Authority, R.E. *Rural Electrification Programme in Kenya*; Rural Electrification Authority: Nairobi, Kenya, 2011.
46. Kaldellis, J.; Kapsali, M.; Kavadias, K. Energy balance analysis of wind-based pumped hydro storage systems in remote island electrical networks. *Appl. Energy* **2010**, *87*, 2427–2437. [CrossRef]
47. Fadare, D.; Irimisose, I.; Oni, A.; Falana, A. Modeling of solar energy potential in Africa using an artificial neural network. *Am. J. Sci. Ind. Res.* **2010**, *1*, 144–157. [CrossRef]
48. Mantis, D.; Hermann, S.; Howells, M.; Welsch, M.; Siyal, S.H. Assessing the technical wind energy potential in Africa a GIS-based approach. *Renew. Energy* **2015**, *83*, 110–125. [CrossRef]

49. Energiewende, A.; Mayer, J.N.; Philipps, S.; Saad, N.; Hussein, D.; Schlegl, T.; Senkpiel, C. Current and future cost of photovoltaics. *Berl. Agora Energiewende* **2015**.
50. Canales, F.A.; Beluco, A. Modeling pumped hydro storage with the micropower optimization model (HOMER). *J. Renew. Sustain. Energy* **2014**, *6*, 043131. [[CrossRef](#)]
51. Kusakana, K. Feasibility analysis of river off-grid hydrokinetic systems with pumped hydro storage in rural applications. *Energy Convers. Manag.* **2015**, *96*, 352–362. [[CrossRef](#)]
52. Bettencourt, E.M.V.; Tilman, M.; Narciso, V.; Carvalho, M.L.S.; Henriques, P.D.S. The livestock roles in the wellbeing of rural communities of Timor-Leste. *Rev. Econ. E Sociol. Rural* **2015**, *53*, 63–80. [[CrossRef](#)]
53. Shahzad, K.; Nasir, A.; Shafiq Anwar, M.; Farid, M.U. Bioenergy Prospective and Efficient Utilization Pattern for Rural Energy Supply in District Pakpattan. *J. Agric. Res.* **2017**, *55*, 101–113.



© 2018 by the authors. Licensee MDPI, Basel, Switzerland. This article is an open access article distributed under the terms and conditions of the Creative Commons Attribution (CC BY) license (<http://creativecommons.org/licenses/by/4.0/>).